# Rashba-type plasmonic metasurface

**Nir Shitrit, Shai Maayani, Dekel Veksler, Vladimir Kleiner, and Erez Hasman***

*Micro and Nanooptics Laboratory, Faculty of Mechanical Engineering and Russell Berrie Nanotechnology Institute, Technion–Israel Institute of Technology, Haifa 32000, Israel*

**Corresponding author: mehasman@technion.ac.il*

Received July 19, 2013; accepted September 12, 2013;
posted September 26, 2013 (Doc. ID 194073); published October 22, 2013

Observation of the plasmonic Rashba effect manifested by a polarization helicity degeneracy removal in a surface wave excitation via an inversion asymmetric metamaterial is reported. By designing the metasurface symmetry using anisotropic nanoantennas with space-variant orientations, we govern the light–matter interaction via the local field distribution arising in a wavelength and a photon spin control. The broken spatial inversion symmetry is experimentally manifested by a directional excitation of surface wave jets observed via a decoupling slit as well as by the quantum dot fluorescence. Rashba-type plasmonic metasurfaces provide a route for spin-based nanoscale devices controlled by the metamaterial symmetry and usher in a new era of light manipulation. 

*OCIS codes:* (160.3918) Metamaterials; (240.0240) Optics at surfaces; (240.5440) Polarization-selective devices; (240.6680) Surface plasmons.

http://dx.doi.org/10.1364/OL.38.004358

The photonic version of the Rashba effect has recently triggered an anomalous interest owing to its physical and technological impact on light–matter interaction control via a metasurface's symmetry [1–3]. The optical Rashba effect (ORE) is a manifestation of the spin–orbit interaction of light [4] under broken inversion symmetry (i.e., the inversion transformation $\mathbf{r} \to -\mathbf{r}$ does not preserve the structure), where the dispersion relation of a metamaterial splits into bands with opposite optical spin (polarization helicity) states [1–3]. Similar to the role of a potential gradient in the electronic Rashba effect [5,6], the space-variant orientation angle $\theta(x, y)$ of optical nanoantennas induces a spin-split dispersion of $\Delta k_R = \sigma \nabla \theta$ [1–3], where $\sigma_\pm = \pm 1$ is the photon spin corresponding to right and left circularly polarized light, respectively. The ORE was observed in the spontaneous emission of anisotropic thermal antenna patterns, such as the quasi one-dimensional (1D) antenna array [1,2] and the inversion asymmetric (IaS) two-dimensional (2D) kagome lattice metamaterial [3]. This effect can be illustrated via a geometric mapping onto the Poincaré sphere [7–13], where the polarization state of light at different locations along the metasurface traverses various geodesic paths arising in the Pancharatnam–Berry phase of $\sigma\theta$ [14,15]; by differentiating the geometric phase, an induced momentum due to polarization rotation is acquired, as originally observed in ultrathin dielectric metamaterials of Pancharatnam–Berry phase optical elements [9–13,16]. This geometric Rashba momentum correction can be either added to or subtracted from the light momentum, owing to its spin-dependent origin. As a result, light–matter interactions governed by momentum selection rules, such as the light coupling to plasmonic metastructures, are perturbed. The resonant coupling of light to surface plasmon polaritons (SPPs) via inversion symmetric metasurfaces is governed by the standard momentum-matching condition and limited by the polarization selectivity so, once the structural parameters are set, the excitation can be tuned by changing the light wavelength or angle of incidence [17]. In addition, ORE-based spinoptical metamaterials offer the photon spin as an additional degree of freedom in nanoscale photonics [1–3,14,15,18–23], holding the promise for controlling SPP excitation with the light's intrinsic angular momentum.

In this Letter, we report on the experimental observation of a Rashba-type plasmonic metamaterial. By designing the metasurface symmetry via space-variant oriented anisotropic nanoantennas, an IaS metastructure was obtained with a Rashba-induced geometric gradient. The spin degeneracy removal in the SPP excitation by the quasi 1D antenna array is based on the spin–orbit momentum-matching (SOMM) condition. This selection rule highlights the spin-controlled additional Rashba momentum in a spinoptical metamaterial. In agreement with a dispersion analysis of the ORE, we observed the directional distribution of plasmonic jets by free-space imaging using a circular decoupling slit as well as the quantum dot (QD) fluorescence. A spin-switch SPP unidirectional guiding in the visible and near-infrared regions under a normal-incidence illumination was presented as a manifestation of broken inversion symmetry. Since we excite different bands in the spin-split dispersion, the excitation of SPP jets depends on both the wavelength and the polarization helicity of the incident light; consequently, for a given wavelength, the excitation is spin-controlled and, by varying the wavelength, the spin-based jets are reversed. Rashba-type plasmonic metasurfaces provide a route for combined polarization- and wavelength-based surface-integrated nanoscale devices via light–matter interactions controlled by the metamaterial symmetry, ushering in a new era of light manipulation.

As a Rashba-type plasmonic metasurface, we considered a 2D periodic metastructure consisting of anisotropic nanoantennas whose local orientation is given by $\theta(x) = \pi x/a$, where $a$ is the rotation period of the structure [see Fig. 1(a)]. The spin-controlled dispersion relation $\omega(k)$ of such an IaS metamaterial [i.e., $\theta(x) \neq \theta(-x)$] obeys the SOMM condition that arises from the combined contributions of the structure and the local field distribution [3]. Accordingly, a SPP jet is excited resonantly when the equation $\mathbf{k}_{\mathbf{in}}^{\parallel}(\sigma) = \mathbf{k}_{\mathbf{SPP}} + m\mathbf{G}_{\mathbf{x}} + n\mathbf{G}_{\mathbf{y}} - \sigma\mathbf{K}_{\mathbf{R},\mathbf{x}}$ is fulfilled. Here, $(\mathbf{G}_{\mathbf{x}}, \mathbf{G}_{\mathbf{y}}) = 2\pi(\hat{\mathbf{x}}/\Lambda_x, \hat{\mathbf{y}}/\Lambda_y)$ are the structural reciprocal vectors corresponding to the local

 

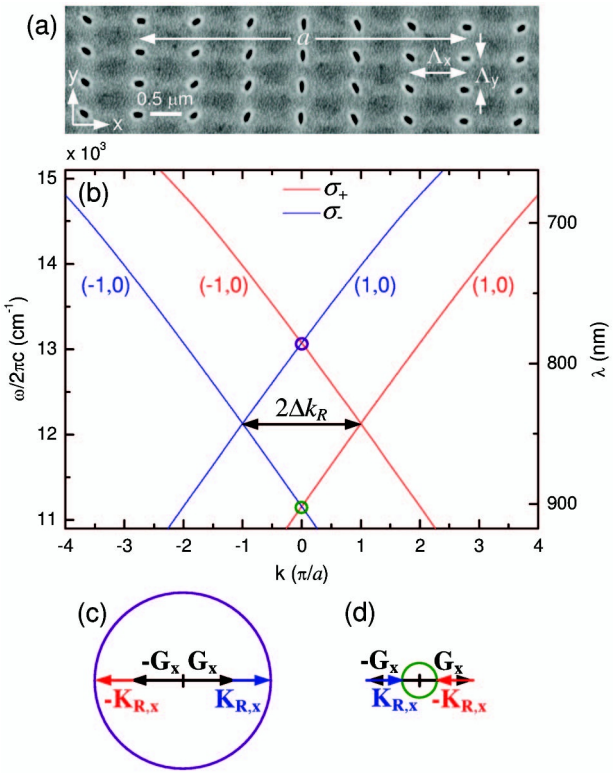


Fig. 1. Rashba-type plasmonic metasurface. (a) Scanning electron microscopy image of the plasmonic quasi 1D antenna array. (b) Calculated spin-projected dispersion in the $x$ direction via the SOMM condition. Red and blue lines correspond to $\sigma_{\pm}$ incident spin states, respectively. Modes are specified with indices $(m, n)$. (c), (d) Vector summation representation of the SOMM condition for the spin-controlled unidirectional excitation at wavelengths of 780 and 870 nm, respectively. Note that $\mathbf{k_{SPP}}$ is the complementary vector for the origin. Purple [in (c)] and green [in (d)] circles correspond to $\mathbf{k_{SPP}}$ circles at high and low frequencies, respectively.

periodicities of $\Lambda_x$ and $\Lambda_y$ [see Fig. 1(a)], whereas $\mathbf{K_{R,x}} = \nabla\theta = \pi\hat{\mathbf{x}}/a$ is the induced geometric Rashba momentum correction; $\mathbf{k}_{\mathbf{in}}^{\parallel}$ is the wavevector of the incident light in the surface plane, $\mathbf{k_{SPP}}$ is the SPP wavevector, and $(m, n)$ are the indices of the radiative modes. By selecting $\Lambda_y$ as a subwavelength scale, the spinoptical metamaterial is considered to be quasi 1D for the spectral region of interest. Regarding low modes of $(m, n) = (\pm 1, 0)$, we calculated the spin-projected dispersion in the IaS direction of the $x$ axis, revealing an optical Rashba spin-split of $|\Delta k_R| = \pi/a$ [Fig. 1(b)]. Such a dispersion reveals two obvious relations: (i) $\omega(k, \sigma_+) = \omega(-k, \sigma_-)$, which is a manifestation of time reversal symmetry; and (ii) $\omega(k, \sigma_+) \neq \omega(k, \sigma_-)$, which is a signature of inversion symmetry violation. At a normal incidence, the free-space resonant wavelengths of the scattered jets are simply calculated via the SOMM condition as $\lambda(m, \sigma) = 2n_{\mathrm{SPP}}N\Lambda_x/(2|m|N \pm \sigma)$. Here, $n_{\mathrm{SPP}} = [\varepsilon_m\varepsilon_d/(\varepsilon_m + \varepsilon_d)]^{1/2}$ is the SPP effective refractive index, where $\varepsilon_m$ and $\varepsilon_d$ are the dispersive dielectric constants of the metal and dielectric, respectively, $N = a/\Lambda_x$ is the level number of rotation, and the $\pm$ sign corresponds to a solution of a SPP jet directed along $\pm x$ axes, respectively. This implies that for a given structure, a directional plasmonic excitation is obtained by switching the spin at a specific wavelength or, alternatively, by varying the wavelength, the spin-based guiding is reversed.

With this in mind, using a focused ion beam (FEI Strata 400s dual beam system, $Ga^+$, 30 keV, 48 pA), we fabricated the plasmonic metasurface consisting of 80 nm × 220 nm rectangular void antennas, etched to a depth of 60 nm upon 200 nm thick gold film, evaporated onto a glass substrate. Local periodicities in $x$ and $y$ directions of $\Lambda_x = 810$ nm and $\Lambda_y = 500$ nm were chosen, respectively, with $N = 6$ [see Fig. 1(a)]. The 60 μm square array was surrounded by a circular slit with a diameter of 180 μm and a width of 100 nm, where only the antenna metasurface was normally illuminated with a continuous wave Ti–sapphire tunable laser (Spectra-Physics 3900S) via a circular polarizer (a linear polarizer followed by a quarter-wave plate). The resonant illuminating wavelengths were set according to the spin-dependent dispersion of this metastructure, calculated via the SOMM condition, verifying the quasi 1D nature in the near-infrared region [Fig. 1(b)]. Propagating SPPs launched by the antenna array and decoupled by the slit were free-space imaged. For the incident wavelength of 780 nm, the plasmonic jets propagating in positive and negative $x$ directions correspond to $\sigma_+$ and $\sigma_-$ spin states, respectively [Figs. 2(b) and 2(a)]. In accordance with the aforementioned prediction, the spin-switch images are reversed for the incident wavelength of 870 nm, and the directed jets are flipped for the same incident polarization helicity by varying the wavelength [Figs. 2(c) and 2(d)]. The spin-controlled nature of the plasmonic

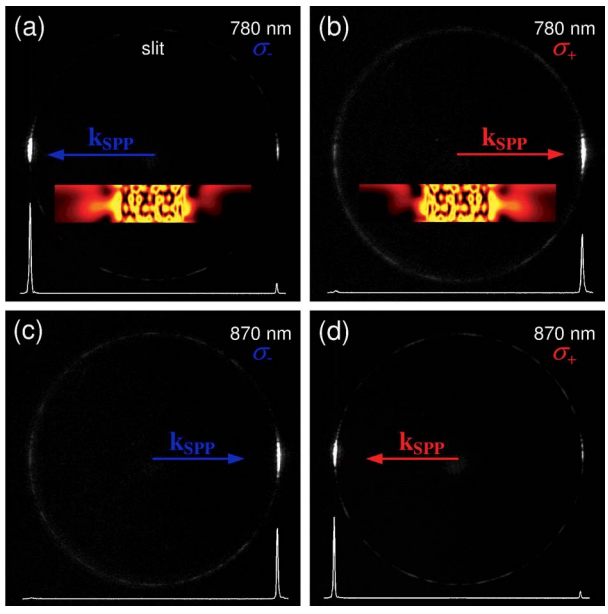


Fig. 2. Observation of the ORE via spin-controlled plasmonics. (a), (b) Measured intensities of unidirectional SPP jets excited by the quasi 1D metasurface and decoupled via the slit for $\sigma_-$ and $\sigma_+$ illuminations, respectively, at a wavelength of 780 nm. Transverse cross sections of the intensity distribution at the center of the slit are depicted by the lines. The insets show finite difference time domain near-field calculations of the normal electric field magnitude. (c), (d) Measured intensities of unidirectional SPP jets for $\sigma_-$ and $\sigma_+$ illuminations, respectively, at a wavelength of 870 nm.

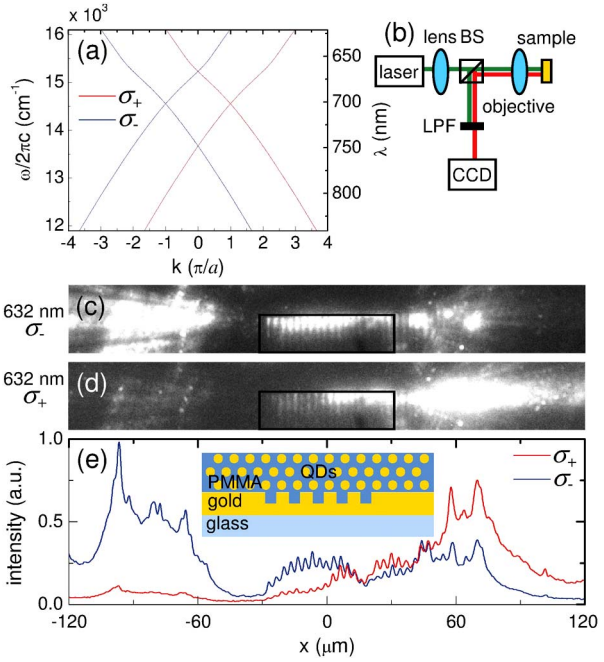


Fig. 3. Fluorescent imaging of the plasmonic Rashba effect. (a) Calculated spin-projected dispersion at the $x$ direction, where the gold-PMMA interface supports SPPs. (b) Fluorescent imaging experimental setup [beam splitter (BS); long-pass filter (LPF)]. (c), (d) Measured intensities of the QD photoluminescence from unidirectional SPP jets for $\sigma_-$ and $\sigma_+$ illuminations, respectively, at a wavelength of 632 nm. The antenna array is depicted by the black frame. (e) Cross sections of the spin-controlled QD photoluminescence along the SPP propagation direction. The inset shows the schematic sample's configuration.

metasurface was also verified by finite difference time domain simulations [Figs. 2(a) and 2(b) insets]. The spin-based launching efficiency was quantitatively estimated by a figure of merit defined as the ratio between the intensities measured in $\pm x$ directions at a specific wavelength and for a specific spin state; the relatively high experimental figures of merit of around 10 indicate an efficient near-infrared spinoptical metamaterial for surface-integrated plasmonic port nanodevices based on the ORE.

The SPP propagation can also be imaged by fluorescent emitters located within the evanescent tail of the plasmon field [24]. We obtained such a fluorescent imaging by coating the metasurface with QDs embedded in a thin polymethyl methacrylate (PMMA) layer. The polymer film thickness of 150 nm was designed in such a way that the metal–polymer interface supports SPPs. In consideration of the interface change, the array's local periodicities were modified to $\Lambda_x = 420$ nm and $\Lambda_y = 330$ nm to match the plasmonic resonance [see Fig. 3(a) for the calculated spin-controlled dispersion relation] to the wavelength region, where the 2.2 nm PbS QD (MKN-PbS-T850) excitation spectrum is relatively high. The metasurface was normally illuminated with a circularly polarized laser beam at a wavelength of 632 nm for the SPP coupling. The excited QD emission was then imaged, while the exciting light was eliminated using a long-pass filter adjusted to the PbS QD peak emission at 850 nm [see Fig. 3(b) for the corresponding experimental setup]. The spin-switch directional plasmonic distribution is shown in Figs. 3(c) and 3(d), where propagating jets in the $\pm x$ directions correspond to an incident spin of $\sigma_\pm$, respectively, similar to the previous observation. Moreover, an advantage of the fluorescent imaging technique is the ability to observe the SPP spatial intensity distribution along the directed propagation.

The geometric Rashba correction in the SOMM condition can be illustrated via the Poincaré sphere, where the polarization state of light traverses a geodesic triangle upon the sphere. This mapping generates a geometric phase term $\phi_g$ equal to half of the solid angle $\Omega$ encompassed by the triangle (see Fig. 4) [7–13]. We consider a circularly polarized light illuminating a plasmonic metasurface consisting of space-variant anisotropic antennas with a local orientation angle of $\theta(x, y)$. In view of the fact that the dipolar field of a locally excited void antenna follows its minor axis [2,20], the in-plane space-variant electric polarizability of the SPPs is represented by a point on the sphere. At different locations along the metasurface the surface wave traverses various geodesic paths on the Poincaré sphere arising in the Pancharatnam–Berry phase of $\sigma\theta$ (see Fig. 4) [14,15]. Alternatively, this geometric phase can be interpreted as a phase delay in the excitation of space-variant anisotropic antennas that are linear polarization selective, where we regard the illuminated circularly polarized light as a rotating-in-time linear polarization [15,21]. By differentiating the generated phase, an induced momentum due to a polarization rotation of $\sigma\nabla\theta$ is acquired. In the context of symmetry, this additional geometrically intrinsic momentum is associated with the optical Rashba spin-split dispersion, which is a manifestation of the spin-orbit interaction

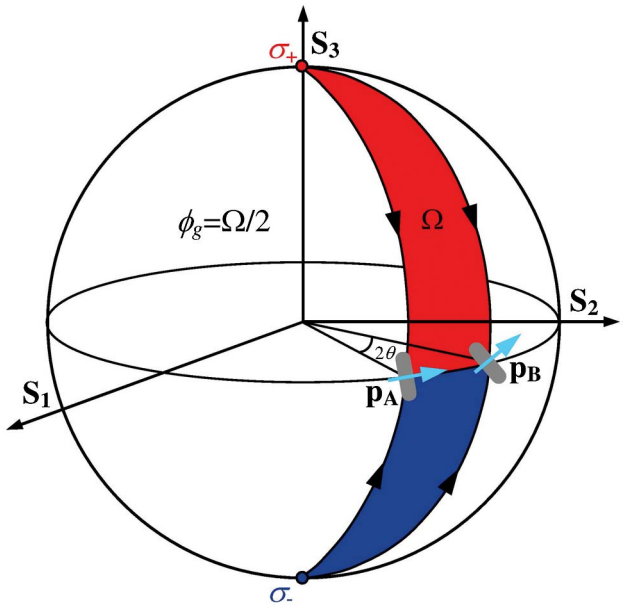


Fig. 4. Illustration of the concept of plasmonic Pancharatnam–Berry phase optical elements. The encompassed area Ω on the Poincaré sphere due to an excitation of space-variant oriented nanoantennas with an electric polarizability **p** generates the geometric phase of $\phi_g$, which arises in the Rashba correction term. Red (top) and blue (bottom) geodesic triangles correspond to incident optical spins of $\sigma_\pm$, respectively.

under broken inversion symmetry [3]. Hence, the introduced quasi 1D spinoptical metamaterial with an IaS direction of $x$ can be regarded as a plasmonic Pancharatnam–Berry phase optical element [9–13,16].

In summary, an optical spin degeneracy removal in a surface wave excitation via an IaS Rashba-type metasurface consisting of rotating anisotropic nanoantennas was presented. The reported phenomenon inspires the development of a unified theory to establish a link between a metasurface symmetry breaking and new selection rules with new degrees of freedom to establish a broader class of light–matter interaction controls. Rashba-type plasmonic metasurfaces provide a route for state-of-the-art spinoptical nanoscale devices that leverage the on-chip photonic nanocircuit platform for information processing and optical communication.

This research was partially supported by the Israel Science Foundationand the Israel Nanotechnology Focal Technology Area on Nanophotonics for Detection.

**References**

1. N. Dahan, Y. Gorodetski, K. Frischwasser, V. Kleiner, and E. Hasman, Phys. Rev. Lett. **105**, 136402 (2010).
2. K. Frischwasser, I. Yulevich, V. Kleiner, and E. Hasman, Opt. Express **19**, 23475 (2011).
3. N. Shitrit, I. Yulevich, E. Maguid, D. Ozeri, D. Veksler, V. Kleiner, and E. Hasman, Science **340**, 724 (2013).
4. V. S. Liberman and B. Y. Zel'dovich, Phys. Rev. A **46**, 5199 (1992).
5. E. I. Rashba, Sov. Phys. Solid State **2**, 1224 (1960).
6. K. Ishizaka, M. S. Bahramy, H. Murakawa, M. Sakano, T. Shimojima, T. Sonobe, K. Koizumi, S. Shin, H. Miyahara, A. Kimura, K. Miyamoto, T. Okuda, H. Namatame, M. Taniguchi, R. Arita, N. Nagaosa, K. Kobayashi, Y. Murakami, R. Kumai, Y. Kaneko, Y. Onose, and Y. Tokura, Nat. Mater. **10**, 521 (2011).
7. S. Pancharatnam, Proc. Indian Acad. Sci. Sect. A **44**, 247 (1956).
8. M. V. Berry, J. Mod. Opt. **34**, 1401 (1987).
9. Z. Bomzon, V. Kleiner, and E. Hasman, Opt. Lett. **26**, 1424 (2001).
10. Z. Bomzon, G. Biener, V. Kleiner, and E. Hasman, Opt. Lett. **27**, 1141 (2002).
11. E. Hasman, Z. Bomzon, A. Niv, G. Biener, and V. Kleiner, Opt. Commun. **209**, 45 (2002).
12. E. Hasman, V. Kleiner, G. Biener, and A. Niv, Appl. Phys. Lett. **82**, 328 (2003).
13. E. Hasman, G. Biener, A. Niv, and V. Kleiner, *Progress in Optics*, E. Wolf, ed. (Elsevier, 2005), Vol. **47**, p. 215.
14. K. Y. Bliokh, Y. Gorodetski, V. Kleiner, and E. Hasman, Phys. Rev. Lett. **101**, 030404 (2008).
15. Y. Gorodetski, A. Niv, V. Kleiner, and E. Hasman, Phys. Rev. Lett. **101**, 043903 (2008).
16. A. V. Kildishev, A. Boltasseva, and V. M. Shalaev, Science **339**, 1232009 (2013).
17. A. Drezet, D. Koller, A. Hohenau, A. Leitner, F. R. Aussenegg, and J. R. Krenn, Nano Lett. **7**, 1697 (2007).
18. O. Hosten and P. Kwiat, Science **319**, 787 (2008).
19. K. Y. Bliokh, A. Niv, V. Kleiner, and E. Hasman, Nat. Photonics **2**, 748 (2008).
20. N. Shitrit, I. Bretner, Y. Gorodetski, V. Kleiner, and E. Hasman, Nano Lett. **11**, 2038 (2011).
21. N. Shitrit, S. Nechayev, V. Kleiner, and E. Hasman, Nano Lett. **12**, 1620 (2012).
22. N. M. Litchinitser, Science **337**, 1054 (2012).
23. X. Yin, Z. Ye, J. Rho, Y. Wang, and X. Zhang, Science **339**, 1405 (2013).
24. H. Ditlbacher, J. R. Krenn, N. Felidj, B. Lamprecht, G. Schider, M. Salerno, A. Leitner, and F. R. Aussenegg, Appl. Phys. Lett. **80**, 404 (2002).